Ocean surface wave evolvement in the Arctic Basin

Vernon A. Squire,[1] Gareth L. Vaughan,[1] and Luke G. Bennetts[1]

Recent basin-scale changes to the compactness and thickness of Arctic sea ice foreshadow that encroaching swells and locally generated waves will exert more influence there in the future. Indeed, it is conceivable that waves may have already hastened the adjustments observed by breaking up ice floes. Yet waves advancing in sea ice attenuate due to being scattered from ice thickness variations and damped by ice inelasticity, turbulence and friction. While past research focuses on scattering by unnaturally perfect features in the ice, the model reported herein assimilates realistic basin-scale swathes of heterogeneous ice and parameterizes damping. By way of example, we show how an ocean wave train evolves during its passage in an 1670-km-long Arctic sea ice profile obtained from submarine.

1. Introduction

Radical changes are occurring in Arctic Basin sea ice because of climate change, a conversion that has global consequences because atmosphere/ocean fluxes attune to the presence of thinner, less compact ice of reduced extent. Coverage has declined by up to 100 000 km^2/year since 1979 [*Vinnikov et al.*, 2006; *Serreze et al.*, 2007] and, in concert, the sea ice has thinned [*Lindsay and Zhang*, 2005; *Kwok and Rothrock*, 2009]. Unquestionably, sea ice adaptation affects our climate system and perturbs a broad range of factors – from altering key elements of the biosphere, to opening shipping routes and influencing other human activities. Moreover, in GCM experiments the Arctic is projected to warm more rapidly than the global average, to become seasonally ice free by the late 21st century.

Although warmer temperatures are a vital determinant of our contemporary eviscerated Arctic, climate change also perturbs many cognate physical processes. Of particular relevance is an increased incidence and intensity of distant storms, which energize higher waves, and the presence of more open water or thinner sea ice, which itself allows greater ingress by waves into the sea ice. Waves are known to fatigue and fracture sea ice [*Langhorne et al.*, 2001] and to encourage melting [*Wadhams et al.*, 1979], but they also penetrate far into the Arctic Ocean and can be created there by wind blowing over ice or by ridging events [*Squire et al.*, 1995; *Squire*, 2007]. Indeed, early Arctic measurements on different ice floes and ice islands suggest that the ice oscillates more or less continuously at 15–60 s period and propagating waves in this band have been identified [*Hunkins*, 1962; *Wadhams and Doble*, 2009]. Large amplitude events have also been felt deep within the pack [*Liu and Mollo-Christensen*, 1988; *Marko*, 2003]. Thus, besides regulating ice morphology and dynamics near the ice margin [*Squire and Moore*, 1980], waves can potentially assist in the annihilation of the sea ice canopy many hundreds of kilometers into the polar interior.

Water waves passing through sea ice are attenuated by the terrain they confront, by natural hysteresis in the ice and by turbulence and friction in the water. Ice terrain is randomly heterogeneous, being composed of open and refrozen leads, pressure ridges and thickness changes arising from convergence and divergence events or uneven growth, melting or snowfall. As a consequence, waves traveling a long way in sea ice experience a sequence of abrupt impedance discontinuities, as multiple irregularities associated with thickness changes are encountered that reflect them. Accordingly, an advancing water wave train slowly evolves by being scattered at and between the many interfaces that signal a change of thickness in the ice terrain. In chorus, it is also damped by dissipative mechanisms that can be parameterized in much the same way as an eddy viscosity is used to capture oceanic turbulence.

We describe how to simulate the scattering and damping of ocean waves in an 'ultra-long' swathe of sea ice terrain, by extending *Vaughan et al.* [2009]. The terrain is real, collected from submarine sonar data, rather than artificial, but ridge sails are found using isostasy [*Mahoney et al.*, 2007]. Of course, sea ice is actually 3 dimensional, with finite sinuous features at oblique angles to the path of wave propagation. This, along with directional spreading, will induce wave energy to leak laterally, especially at shorter periods. Although the model can actually treat oblique incidence, here a long-crested wave train is taken to impinge normally on features in the ice – so the analysis is 2 dimensional. A 1670-km-long central Arctic sea ice profile is used to demonstrate the method.

2. Arctic Sea Ice Topography

From 1975–2000 US and Royal Navy nuclear submarines conducted cruises in the Arctic Basin to profile the underside of the perennial sea ice by means of upward-pointing sonar. These data are available from the National Snow and Ice Data Center [*NSIDC*, 2006] as downloadable files, each of which contains roughly 50 km of ice-drafts at 1 m intervals, processed to remove the influence of varying submarine speed and elevation. Files are also terminated where a significant change of course occurs or where dropout causes gaps of more than 250 m. Artificial data that conform to the statistics of the transect can be used to fill gaps (see Appendix).

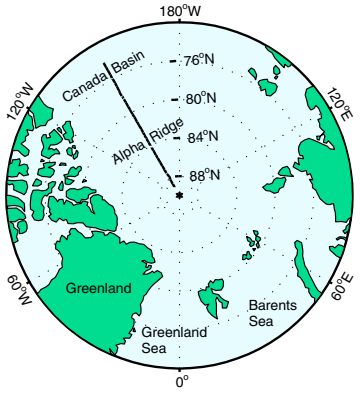

Figure 1. The Arctic Ocean and a portion of the submarine track during collection of the 1994 *NSIDC* [2006] data set.

Thirty four transects located near a great-circle track that delineate a single ultra-long swathe of roughly 1670 km, when conjoined, have been selected from 85 files available from a 1994

[1]Department of Mathematics and Statistics, University of Otago, P. O. Box 56, Dunedin 9054, New Zealand.

0094-8276/09/$5.00

cruise. The composite profile is fenestrated by numerous gaps, the longest being 22.3 km. Starting just beyond the pole, the submarine track crosses the Alpha Ridge (2.7 km minimum depth) and then traverses the roughly 4-km-deep Canada Basin (Figure 1). The profile is assumed to be parallel to the principal direction of wave propagation, as the prevailing swells that enter the Arctic Ocean travel north from the Greenland and Barents Seas in an approximately 60° sector drawn from the pole. Taking each draft to represent a 1-m-long section of sea ice of constant thickness [*Vaughan et al.*, 2009], the profile is plotted in Figure 2a with gaps filled, while Figure 2c details 10 km of profile using a value of 5 for the ratio of draft to upper surface elevation (see Appendix). Computational workload is eased by using 'block averaging' to reduce the number of drafts (see Appendix), as the precision and frequency of data points is unnecessarily high in the raw files.

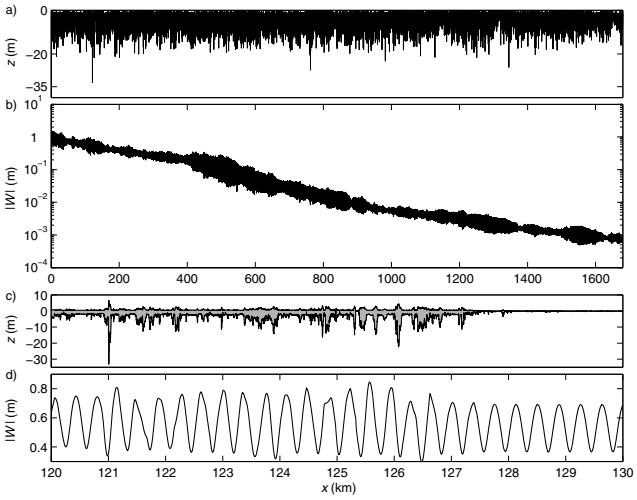

Figure 2. (a) The draft profile from the 1994 *NSIDC* [2006] data with all gaps filled; (b) the magnitude of the vertical displacement $|W|$ of a 22 s ocean wave train as it progresses through ice terrain for the entire 1670 km transect; (c) a 10 km example of the thickness profile used in the model, showing ridge sails and keels; and (d) 10 km detail of the displacement magnitude $|W|$. Each are plotted against the horizontal coordinate x.

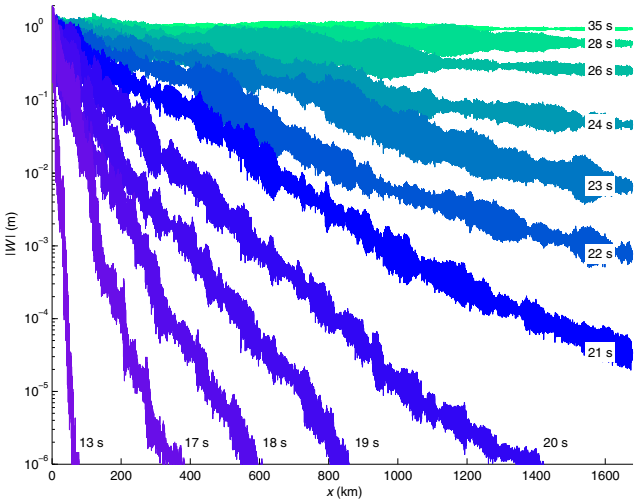

Figure 3. How the amplitude of ocean waves with T ranging from 13 to 35 s is affected by 1670 km of ice terrain.

3. Modeling Wave Scattering and Damping

Bennetts et al. [2007] and *Vaughan et al.* [2009] provide more details about the theory that undergirds this work. In brief, we use linear wave theory and model the sea ice as a spatially variable, thin flexible plate with an ancillary viscosity term, and express a velocity potential as an eigenfunction expansion where the sea ice has constant thickness (see Appendix).

A sea ice profile, comprising S drafts of differing lengths, is placed between two semi-infinite plates having drafts d_0 and d_{S+1}. An exponentially decaying surface wave propagates in the left plate towards the profiled ice such that at $x = 0$, where that plate abuts the profile, it has unit amplitude. At a discontinuity in the thickness of the ice, waves proportional to $e^{\pm ik_n x}$ are induced on each side of the feature that then interact with other ice sheet irregularities. We use a multi-mode approximation [*Bennetts et al.*, 2007] to extract the amplitudes of these waves during these embrangled interactions, but applied on segmented profiles [*Vaughan et al.*, 2009] because a direct implementation is numerically impractical for the required number of modes N when S is large.

4. Results

Figure 2b shows how a 22 s ocean wave advances through the 1670 km of irregular Arctic sea ice plotted in Figure 2a. Scattering and dissipation is very evident, although the latter is modest as the value of dynamic viscosity is small ($0.1\,\mathrm{Pa\,s\,m^{-1}}$). During its passage along the transect, wave amplitude reduces exponentially by about 3 decades – the curve's fine structure being caused by scattering interactions between leads and pressure ridges. These can be seen in the 10 km multifaceted section of icescape terrain of Figure 2c, which includes a ∼35 m keel and a stretch of refrozen lead from 128–130 km. The modulation of the wave due to the variability it confronts in this section appears in Figure 2d, where the oscillation is strikingly constant across the refrozen lead though the effect of the deep keel is more subtle.

Because of attenuation, ocean waves reaching well into the Arctic Basin are normally of long period, so we are interested in mapping how these waves progress from their point of entry or nascency. This is explored in Figure 3 for our exemplar ice terrain at periods T from 13–35 s, where the exponential decay reduces as period increases. Fine structure variability is due to waves being scattered to-and-fro from heterogeneity, as before. High decay

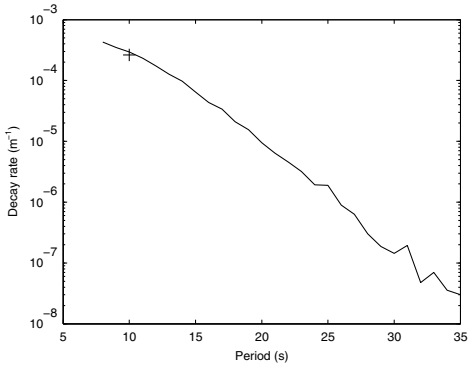

Figure 4. The rate of decay (attenuation coefficient, α) as a function of T. The cross plotted just below the curve at $T = 10$ s shows α when viscosity $\gamma = 0$, i.e. when the decay is all due to scattering.

rates characterize the shortest periods computed, e.g. only 5% of the amplitude of a 10-s-period wave remains after 10 km are traveled, while 50% remains at 15 s. A 22 s wave can travel 1000 km before it is reduced to 2% of its original amplitude. For a site positioned well within the Arctic, the upshot is a distorted oncoming wave energy spectrum that includes only the longest oscillations, in accord with deep Arctic experience [*Hunkins*, 1962; *Wadhams and Doble*, 2009].

Crucial to our understanding of how ocean waves communicate with Arctic Basin sea ice is how the attenuation coefficient α depends on T. This is shown in Figure 4, where α is deduced from a least squares fit to the curves in Figure 3, recognizing that any conclusions reached will be statistically robust because the prototype transect is ultra-long. Figure 4 furnishes an unexpected result, namely that α is itself more or less exponential in T for periods above about 10 s, with the hint of a 'roll-over' [see *Wadhams et al.*, 1988] as shorter periods are approached from the right. To be specific $\alpha(T) = 0.02\exp(-0.386\,T)$, which should be representative of Arctic Basin sea ice at the date collected, but which will overestimate attenuation now that the Arctic Basin sea ice is thinner. (The 30% thinner, 2007 sea ice reported by *Wadhams and Doble* [2009], produces a roughly 18% reduction in α at $T = 15$ s.)

5. Discussion and Conclusions

The novelty of this work is in our application of technical mathematics to a complicated heterogeneous natural phenomenon using real ice draft observations collected in the Arctic Ocean by submarine. By this means, the way in which ocean waves propagate in an ultra-long sea ice transect has been successfully studied for the first time, without recourse to contrived assumptions about the properties of the ice sheet topography. As in the marginal ice zone [*Squire and Moore*, 1980; *Wadhams et al.*, 1988], we find that the waves attenuate exponentially with distance traveled, but with an attenuation coefficient that also depends exponentially on wave period. In a properly 3 dimensional exposition, energy would leak from the forward traveling wave vector because of oblique scattering, but it is currently impossible to quantify this without basin-scale ice thickness maps. Beyond the current generation of models, we expect that subsuming 3 dimensionality over large scales would induce greater decay rates than those observed in the results of this work.

The primary catalyst for this study is the onset of climate change, where waves are expected to play an increased role in the despoilment of the polar ice cover. A second impetus is the realization that penetrating ocean waves can be effective in monitoring ice thickness [*Nagurny et al.*, 1994; *Wadhams and Doble*, 2009; *Williams and Squire*, 2009 in press]. A third relates to the operational use of Arctic waters by the hydrocarbon and offshore engineering industries, as pervasive ocean waves engender an additional hazard in this harsh environment. And a fourth concerns outcomes that bring us closer to properly integrating wave/ice interaction into GCMs.

Appendix: Methods

Vaughan et al. [2009] use an autocorrelation technique devised by D. Percival (personal communication, 2008) to fill gaps inside sonar transects with 'Gaussianized' sections. The same method is employed here but we must now also fill gaps between different files, which is more computationally demanding as the gaps can be long and gap-filling requires Cholesky decomposition of a matrix with size equal to the gap length in meters. This imposes a limit on the gap that may be filled (22.3 km for a computer with 8 Gb of RAM).

The elevation of the upper surface of the sea ice cannot be measured with upward pointing sonar, so to convert draft to ice thickness the ratio of draft to this elevation is taken to be a constant. A ratio of 5 is assumed, consentient with the range of values 4.5–9 reported in the literature [*Mahoney et al.*, 2007].

In block averaging [*Vaughan et al.*, 2009] a value is first chosen for δ. Then, starting with the first draft d_1, subsequent drafts that lie within $d_1 \pm \delta$ are counted, averaged and replaced by the single average value over an equivalent length. By this means long stretches of sea ice with inconsequential thickness variations are replaced by uniform sections, reducing the number of drafts required to describe the profile and expediting solution. The smaller δ is taken, the more accurate the profile and the more precise the solution.

Expressed as an eigenfunction expansion the solution has an infinite number of terms that involve $\exp(\pm ik_n x)$, such that $k = k_n$ satisfies the dispersion relation

$$\left(1 - \mu\frac{4\pi^2}{gT^2} + \beta k^4 - i\gamma\right) k \tanh k(h-d) = \frac{4\pi^2}{gT^2},$$

where μ is mass per unit length, g is acceleration due to gravity, β is flexural rigidity, h is ocean depth, and d is ice draft. (Open water dispersion is recovered when $\mu = \beta = \gamma = d = 0$.) Roots k_n must be evaluated for every draft in the profile at each frequency but, because the k_n become less significant as n increases, the series is truncated after finite N terms. The viscosity term, $i\gamma$, incorporates an aggregation of dissipative mechanisms. If $\gamma = 0$, the set $\{k_n\}$ contains a real root, two complex roots and a countable infinity of imaginary roots; $-k_n$ are also roots, being waves traveling in the opposite direction. If $\gamma > 0$, the k_n are all complex, the previously real root now designating a propagating sinusoidal wave with superimposed exponential decay.

To segment a profile it is split into 2 parts, for which solutions are found and from which the solution for the whole profile is constructed. An optimal number of subdivisions minimizes solution time but, when the ice profile is very long, it is advantageous to nest segmentation over more than one layer. For the ultra-long profile of Figures 1 and 2a we use 4 layers, with segments chosen to keep solution times low. This innovation decreases memory requirements and the layered structure of the algorithm facilitates the implementation of a coherent system for data transfer.

Acknowledgments. Supported by the Marsden Fund Council, from Government funding administered by the Royal Society of New Zealand, and by the University of Otago.

References

Bennetts, L. G., N. R. T. Biggs, and D. Porter (2007), A multi-mode approximation to wave scattering by ice sheets of varying thickness, *J. Fluid Mech.*, *579*, 413–443.

Hunkins, K. (1962), Waves on the Arctic Ocean, *J. Geophys. Res.*, *67*(6), 2477–2489.

Kwok, R., and D. A. Rothrock (2009), Decline in Arctic sea ice thickness from submarine and ICESat records: 1958–2008, *Geophys. Res. Lett.*, *36*, L15501, doi:10.1029/2009GL039035.

Langhorne, P. J., V. A. Squire, and T. G. Haskell (2001), Lifetime estimation for a fast ice sheet subjected to ocean swell, *Ann. Glaciol.*, *33*, 333–338.

Lindsay, R. W., and J. Zhang (2005), The thinning of Arctic sea ice, 1988–2003: Have we passed a tipping point?, *J. Climate*, *18*, 4879–4894.

Liu, A. K., and E. Mollo-Christensen (1988), Wave propagation in a solid ice pack, *J. Phys. Oceanogr.*, *18*(11), 1702–1712.

Mahoney, A., H. Eicken, and L. Shapiro (2007), How fast is landfast sea ice? A study of the attachment and detachment of nearshore ice at Barrow, Alaska, *Cold Reg. Sci. Technol.*, *47*, 233–255.

Marko, J. R. (2003), Observations and analyses of an intense waves-in-ice event in the Sea of Okhotsk, *J. Geophys. Res.*, *108*(C9), 3296, doi:10.1029/2001JC001214.

Nagurny, A. P., V. G. Korostolev, and V. P. Abaza (1994), A method for determination of effective sea ice thickness in the Arctic basin for climate monitoring, *Bull. Russian Acad. Sci. Phys. Suppl. Phys. Vib.*, *58*, 168–174.

NSIDC (2006), Submarine upward looking sonar ice draft profile data and statistics, `http://nsidc.org/data/g01360.html`.

Serreze, M. C., M. M. Holland, and J. Stroeve (2007), Perspectives on the Arctic's shrinking sea-ice cover, *Science*, *315*(5818), 1533–1536.

Squire, V. A. (2007), Of ocean waves and sea-ice revisited, *Cold Reg. Sci. Technol.*, *49*(2), 110–133.

Squire, V. A., and S. C. Moore (1980), Direct measurement of the attenuation of ocean waves by pack ice, *Nature*, *283*(5745), 365–368.

Squire, V. A., J. P. Dugan, P. Wadhams, P. J. Rottier, and A. K. Liu (1995), Of ocean waves and sea ice, *Annu. Rev. Fluid Mech.*, *27*, 115–168.

Vaughan, G. L., L. G. Bennetts, and V. A. Squire (2009), The decay of flexural-gravity waves in long sea ice transects, *Proc. R. Soc. A*, *465*(2109), 2785–2812.

Vinnikov, K. Y., D. J. Cavalieri, and C. L. Parkinson (2006), A model assessment of satellite observed trends in polar sea ice extents, *Geophys. Res. Lett.*, *33*, L05704, doi:10.1029/2005GL025282.

Wadhams, P., and M. J. Doble (2009), Sea ice thickness measurement using episodic infragravity waves from distant storms, *Cold Reg. Sci. Technol.*, *56*(2–3), 98–101.

Wadhams, P., A. E. Gill, and P. F. Linden (1979), Transects by submarine of the East Greenland Polar Front, *Deep-Sea Res.*, *26A*(12), 1311–1327.

Wadhams, P., V. A. Squire, D. J. Goodman, A. M. Cowan, and S. C. Moore (1988), The attenuation of ocean waves in the marginal ice zone, *J. Geophys. Res.*, *93*(C6), 6799–6818.

Williams, T. D., and V. A. Squire (2009 in press), On the estimation of ice thickness from scattering observations, *Dynam. Atmos. Oceans*, doi: 10.1016/j.dynatmoce.2009.08.001.

Vernon A. Squire, Department of Mathematics and Statistics, University of Otago, P. O. Box 56, Dunedin 9054, New Zealand. (vernon.squire@otago.ac.nz)

Gareth L. Vaughan, Department of Mathematics and Statistics, University of Otago, P. O. Box 56, Dunedin 9054, New Zealand.

Luke G. Bennetts, Department of Mathematics and Statistics, University of Otago, P. O. Box 56, Dunedin 9054, New Zealand.